Experimental demonstrations of 30Gb/s/ digital orthogonal filtering-multiplexed multiple channel transmissions over IMDD PON systems utilizing 10G-class optical devices

Deng, Mingliang; Sankoh, Abdulai; Giddings, Roger; Tang, Jianming

Optics Express

DOI:
10.1364/OE.25.024251

Published: 25/09/2017

Publisher's PDF, also known as Version of record

Research Article | Vol. 25, No. 20 | 2 Oct 2017 | OPTICS EXPRESS 24251
Optics EXPRESS

Experimental demonstrations of 30Gb/s/λ digital orthogonal filtering-multiplexed multiple channel transmissions over IMDD PON systems utilizing 10G-class optical devices

M. L. DENG,* A. SANKOH, R. P. GIDDINGS, AND J. M. TANG

School of Electronic Engineering, Bangor University, Bangor, LL57 1UT, UK
**m.deng@bangor.ac.uk*

Abstract: By utilizing digital orthogonal filtering (DOF) in the digital domain, we report, for the first time, experimental demonstrations of aggregated 30.078Gb/s/λ transmissions of DOF-multiplexed spectrally-overlapped and/or frequency gapless six channels over IMDD PON systems incorporating off-the-shelf and low-cost 10G-class optical devices. Experimental results show that simple adaptive channel power loading implemented in the digital domain enables very similar transmission performances of individual channels regardless of their locations in the digital filter space. As a direct result of the interplay between the transmission system-associated negative chromatic dispersion and the intensity modulation-induced frequency chirp, negative power penalties of >0.2dB are experimentally observed for all the involved channels under various transmission system configurations. In addition, excellent performance robustness of the demonstrated systems is also obtainable for various transmission distances up to 45km.

OCIS codes: (060.2330) Fiber optics communications; (060.4230) Multiplexing; (060.4080) Modulation.

References and links

1. D. Nesset, "The PON roadmap," in *Optical Fiber Communication/National Fiber Optic Engineers Conference* (OFC/NFOEC, 2016), paper W4C.1.
2. N. Cvijetic, A. Tanaka, P. Ji, K. Sethuraman, S. Murakami, and T. Wang, "SDN and OpenFlow for dynamic flex-grid optical access and aggregation networks," J. Lightwave Technol. **32**(4), 864–870 (2014).
3. G. Talli, F. Slyne, S. Porto, D. Carey, N. Brandonisio, A. Naughton, P. Ossieur, S. McGettrik, C. Blumm, M. Ruffini, D. Payne, R. Bonk, T. Pfeiffer, N. Parsons, and P. Townsend, "SDN enabled dynamically reconfigurable high capacity optical access architecture for converged services," J. Lightwave Technol. **35**(3), 550–560 (2017).
4. J. E. Mitchell, "Integrated wireless backhaul over optical access networks," J. Lightwave Technol. **32**(20), 3373–3382 (2014).
5. X. Liu and F. Effenberger, "Emerging optical access network technologies for 5G wireless," J. Opt. Commun. Netw. **8**(12), B70–B79 (2016).
6. Y. Luo, B. Lin, H. Yang, J. Li, Y. He, Z. Chen, and Z. Li, "Symmetic 100-Gb/s TWDM-PON with DSB OFDM Modulation," in *Optical Fiber Communication/National Fiber Optic Engineers Conference* (OFC/NFOEC, 2014), paper W2A.61.
7. V. Houtsma and D. V. Veen, "Demonstration of symmetrical 25 Gbps TDM-PON with 31.5 dB optical power budget using only 10 Gbps optical components," in *European Conference on Optical Communication* (ECOC, 2015), paper PDP.4.3.
8. J. Wei, N. Eiselt, H. Griesser, K. Grobe, M. H. Eiselt, J. J. Vegas Olmos, I. Tafur Monroy, and J.-P. Elbers, "Demonstration of the first real-time end-to-end 40-Gb/s PAM for next-generation access applications using 10-Gb/s transmitter," J. Lightwave Technol. **34**(7), 1628–1635 (2016).
9. Z. Li, L. Yi, X. Wang, and W. Hu, "28 Gb/s duobinary signal transmission over 40 km based on 10 GHz DML and PIN for 100 Gb/s PON," Opt. Express **23**(16), 20249–20256 (2015).
10. Ye, S. Li, N. Cheng, and X. Liu, "Demonstration of high-performance cost-effective 100-Gb/s TWDM-PON using 4×25-Gb/s optical duobinary channels with 16-GHz APD and receiver-side post equalization," European Conference on Optical Communication (ECOC, 2015), paper Mo.3.4.4.
11. H. Ji, L. Yi, Z. Li, L. Xue, X. Li, Q. Yang, S. Wang, Y. Yang, S. Yu, and W. Hu, "Field demonstration of a real-time 100Gb/s PON based on 10G-class optical devices," J. Lightwave Technol. **35**(10), 1914–1921 (2017).

#300625 https://doi.org/10.1364/OE.25.024251
Journal © 2017 Received 22 Jun 2017; revised 17 Sep 2017; accepted 18 Sep 2017; published 25 Sep 2017
Corrected: 18 October 2017

Optics EXPRESS

12. M. Bolea, R. P. Giddings, and J. M. Tang, "Digital orthogonal filter enabled optical OFDM channel Multiplexing for software-reconfigurable elastic PONs," J. Lightwave Technol. **32**(6), 1200–1206 (2014).
13. M. Bolea, R. P. Giddings, M. Bouich, C. Aupeti-Berthelemot, and J. M. Tang, "Digital filter multiple access PONs with DSP-enabled software reconfigurability," J. Opt. Commun. Netw. **7**(4), 215–222 (2015).
14. Y. Dong, E. Rawachy, R. P. Giddings, W. Jin, D. Nesset, and J. M. Tang, "Multiple channel interference cancellation of digital filter multiple access PONs," J. Lightwave Technol. **35**(1), 34–44 (2017).
15. E. Al-Rawachy, R. P. Giddings, and J. M. Tang, "Experimental demonstration of a DSP-based cross-channel interference cancellation technique for application in digital filter multiple access PONs," Opt. Express **25**(4), 3850–3862 (2017).
16. S. K. Ibrahim, J. Zhao, D. Rafique, J. A. O'Dowd, and A. D. Ellis, "Demonstration of world-first experimental optical fast OFDM system at 7.174 Gbit/s and 14.348 Gbit/s," in *European Conference on Optical Communication* (ECOC, 2010), pp 1–3.
17. E. Giacoumidis, S. K. Ibrahim, J. Zhao, J. M. Tang, I. Tomkos, and A. D. Ellis, "Experimental demonstration of cost-effective intensity-modulation and direct-detection optical fast-OFDM over 40km SMF transmission," in *Optical Fiber Communication/National Fiber Optic Engineers Conference* (OFC/NFOEC, 2012), paper JW2A.65.
18. W. Jin, X. Duan, Y. Dong, B. Cao, R. P. Giddings, C. F. Zhang, K. Qiu, and J. M. Tang, "DSP-enabled flexible ROADMs without optical filters and O-E-O conversions," J. Lightwave Technol. **33**(19), 4124–4131 (2015).
19. G. H. Im, D. D. Harman, G. Huang, A. V. Mandzik, M. H. Nguyen, and J. J. Werner, "51.84 Mb/s 16-CAP ATM LAN standard," J. Sel. Areas Commun. **13**(4), 620–632 (1995).
20. M. L. Deng, Y. Ling, X. F. Chen, R. P. Giddings, Y. H. Hong, X. W. Yi, K. Qiu, and J. M. Tang, "Self-seeding-based 10Gb/s over 25km optical OFDM transmissions utilizing face-to-face dual-RSOAs at gain saturation," Opt. Express **22**(10), 11954–11965 (2014).
21. Y. Gao, Q. Zhuge, W. Wang, X. Xu, J. M. Buset, M. Qiu, M. Morsy-Osman, M. Chagnon, F. Li, L. Wang, C. Lu, A. P. T. Lau, and D. V. Plant, "40 Gb/s CAP32 short reach transmission over 80 km single mode fiber," Opt. Express **23**(9), 11412–11423 (2015).
22. X. Zheng, X. Q. Jin, R. P. Giddings, J. L. Wei, E. Hugues-Salas, Y. H. Hong, and J. M. Tang, "Negative power penalties of optical OFDM signal transmissions in directly modulated DFB laser-based IMDD systems incorporating negative dispersion fibers," IEEE Photonics J. **2**(4), 532–544 (2010).

1. Introduction

Fueled by a wide diversity of bandwidth-hungry applications such as high-definition TV, cloud computing, video-on-demand, the rapidly increasing number of mobile users and their various emerging services, the data bandwidth demand for broadband services continues to rise considerably. As a direct result, there is a tangible need for enhancing both the signal transmission capacities and the networking functionalities of next-generation passive optical networks (NG-PONs) whilst still maintaining their cost-effectiveness due to the cost-sensitive nature of the access networks [1]. Moreover, since the quickly growing number of mobile users is the dominant driving force of the unprecedented bandwidth requirement, data traffic patterns are also becoming increasingly dynamic. This causes significant challenges for efficient bandwidth provision and network management. It is, therefore, critical to equip NG-PONs with the software defined networking (SDN)-based network operation capability to offer highly desirable networking functionalities, including adaptability, flexibility, reconfigurability, elasticity and backwards compatibility [2,3]. Furthermore, to further improve the dynamic network operation functionalities and cost effectiveness, as well as the efficiency in both bandwidth utilization and network management, the seamless convergence of traditional optical access networks, metropolitan area networks, and 4G/5G mobile front-haul/back-haul networks is also highly preferred to form integrated cloud access networks for implementing sustainable "future-proof" optical access networks [4,5].

To meet the increasing transmission capacity demand in a cost-effective manner, extensive research has been carried out for further upgrade of the newly standardized NG-PON (NG-PON2 that delivers 40Gb/s downstream transmissions by stacking four 10Gb/s wavelength channels over power-split optical distribution networks) to an aggregated transmission capacity of 100Gb/s with 25Gb/s per wavelength. Example experimental demonstrations of 25Gb/s single-wavelength intensity-modulation and direct-detection (IMDD)-based transmission systems have been reported using signal modulation formats including double sideband orthogonal frequency division multiplexing (DSB-OFDM) [6], four-level pulse amplitude modulation (PAM-4) [7,8], electrical/optical duobinary [9,10], and

Optics EXPRESS

non-return-to-zero on-off-keying (NRZ-OOK) [11]. These schemes have demonstrated the feasibility of utilizing 10G-class optical devices to support 25Gb/s single-wavelength signal transmission capacity. From the cost point of view, this offers a promising technical strategy for practical implementation.

On the other hand, to improve the software-controllable network reconfigurability and network bandwidth utilization efficiency, by making use of digital orthogonal filtering (DOF) implemented with hardware-based digital signal processing (DSP), we have recently proposed and theoretically investigated a novel channel multiplexing/demultiplexing technique [12], in which centralized SDN controller-managed, software-reconfigurable digital orthogonal filters are embedded in transceivers to adaptively and dynamically combine and separate different digital signal channels according to channel spectral characteristics and network traffic status. It has been shown [12–15] that the proposed DOF-based multiplexing/demultiplexing technique not only provides the PON systems with the aforementioned online network operation functionalities, but also has the excellent potential of achieving the integrated cloud access networks, because of its salient advantages listed below:

- Offering excellent DSP-enabled network reconfigurability, flexibility and elasticity. In comparison with other multiplexing/demultiplexing schemes based on cost-effective advanced signal modulation techniques such as fast OFDM [16,17], the DOF-based multiplexing/demultiplexing technique possesses inherent network operation transparency to major system/network design characteristics including, for example, signal modulation formats, transmission bandwidths and detection schemes.
- Fully supporting the conventional SDN solution and further extending the solution to the physical layer because of the implementation of software-reconfigurable DSP functions in the involved optical transceivers.
- Significantly improving the transmission spectral efficiency as the gapless aggregation of multiple signals of various characteristics can be achievable.
- Enabling DOF-based online channel aggregation in the electrical/optical domain without requiring extra analogue components, and also channel add/drop functions in network nodes when using our recently proposed flexible reconfigurable optical add/drop multiplexers [18]. The DOF-based operations introduce negligible latency.

Form the above descriptions, it is easy to understand that, to equip 100Gb/s NG-PONs with the aforementioned advantageous network functions, it is greatly beneficial if the DOF-enabled multiplexing/demultiplexing technique can be employed in 25Gb/s single-wavelength IMDD PON transmission systems incorporating 10G-class optical devices.

In this paper, by making use of off-the-shelf 10G-class optical devices, we report, for the first time, experimental demonstrations of aggregated 30.078Gb/s/λ signal transmissions over >25km single-mode fiber (SMF) multi-channel IMDD PON systems, where six independent channels are multiplexed/demultiplexed utilizing digital orthogonal filters in the digital domain. The experimental results show that the achievable signal transmission capacity is mainly determined by the chromatic dispersion-induced power fading effect rather than digital filter frequency response characteristics. As a direct result, when adaptive channel power loading is applied, the channel spectral location-independent transmission performance with a negative power penalty of >0.2dB can be obtained for all the involved channels. In addition, excellent performance robustness of the demonstrated systems is also experimentally observed for different transmission distances up to 45km.

Optics EXPRESS

2. DOF-enabled channel multiplexing/demultiplexing and experimental system setup

2.1 Operating principles of DOF-enabled channel multiplexing/demultiplexing

As a detailed theoretical analysis of the DOF-enabled channel multiplexing/demultiplexing technique has already been presented in [12], only the basic operation principles are outlined below. As shown in Fig. 1, *N* independent channels are multiplexed/demultiplexed utilizing DSP-based digital orthogonal filters embedded in the optical transceivers. At the transmitter side, each individual channel's data is first digitally encoded by an arbitrary signal modulation format such as OFDM, PAM and NRZ-OOK. The encoded sample sequence is then up-sampled by a factor of *M* by inserting *M*-1 zeros between two consecutive samples, and subsequently the up-sampled sequence passes through a digital orthogonal shaping filter. As a result, an orthogonal channel is generated at the output of the shaping filter. All of the generated orthogonal channels are added together in the digital domain and are input into a single digital-to-analogue converter (DAC). The resulting analog signal emerging from the DAC is then fed to an optical intensity modulator and the optical signal is launched into a fiber transmission link. At the receiver side, the optical signal is electrically converted and then digitalized by an analog-to-digital converter (ADC). After that, the digitalized electrical signal is split equally to feed *N* parallel receiver modules, where the digital signal is filtered by a corresponding matching filter to demultiplex the desired channel. The digitally filtered channel is down-sampled by a factor of *M* by selecting every M^{th} sample from the sample sequence. Finally, the demultiplexed channel is recovered after signal decoding.

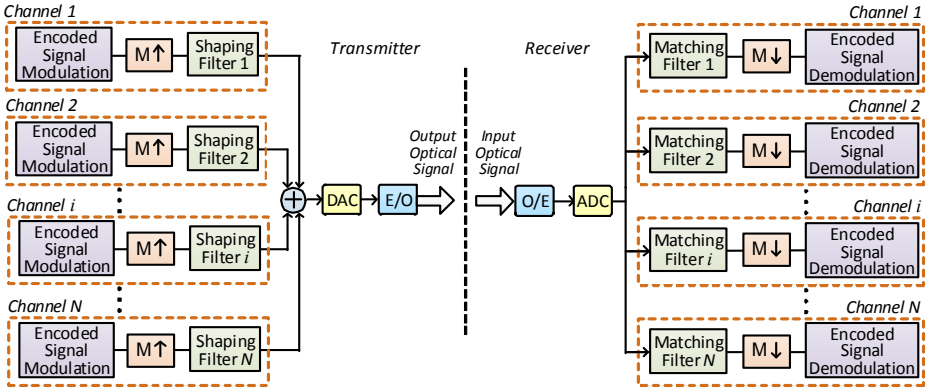

Fig. 1. Schematic diagram of the transceivers utilizing digital orthogonal filtering-enabled channel multiplexing/demultiplexing.

To implement DOF-enabled channel multiplexing/demultiplexing, use can be made of the Hilbert-pair approach [19] to construct the required digital orthogonal filters. The impulse responses of the *i*th Hilbert-pair, $h_i(t)$, are given by

$$\begin{aligned} h_i^I(t) &= p(t)\cos(2\pi f_{ci}t), \\ h_i^Q(t) &= p(t)\sin(2\pi f_{ci}t), \end{aligned} \tag{1}$$

where f_{ci} corresponds to the central frequency of the *i*th Hilbert-pair, and $p(t)$ is the baseband pulse with a square-root raised-cosine form expressed as

$$p(t) = \frac{\sin\left[\pi(1-\alpha)t'\right] + 4\alpha t'\cos\left[\pi(1+\alpha)t'\right]}{\pi t'\left[1-(4\alpha t')^2\right]}, \quad t' = \frac{t}{T} \tag{2}$$

Optics EXPRESS

where T is the sample period prior to up-sampling and α factor controls the excess of bandwidth of the square-root raised-cosine function. The superscripts "I" and "Q" denote the spectrally-overlapped in-phase and quadrature-phase components of the Hilbert-pair respectively. Each of these components can be independently used as the impulse response of an individual shaping filter. Whilst the impulse responses of the matching filters can be written as the time reversals of the corresponding shaping filters, $m_i(t)$:

$$\begin{aligned} m_i^I(t) &= h_i^I(-t), \\ m_i^Q(t) &= h_i^Q(-t), \end{aligned} \tag{3}$$

with

$$m_i^A(t) \otimes h_j^B(t) = \begin{cases} \delta(t-t_0) & A = B \text{ and } i = j \\ 0 & A \neq B \text{ or } i \neq j \end{cases} \tag{4}$$

where the superscripts A and B each indicates I or Q, and t_0 denotes the time delay caused by the digital filtering process. For multiplexing/demultiplexing N independent channels, the up-sampling factor, M, should satisfy $M \geq N$ [12]. In addition, the central frequency of the digital orthogonal filters, f_{ci}, is given by

$$f_{ci} = (2i-1)\frac{f_{DAC/ADC}}{4M}, \quad i = 1, 2, ..., M, \tag{5}$$

where $f_{\mathrm{DAC/ADC}}$ is the sampling speed of the DAC/ADC.

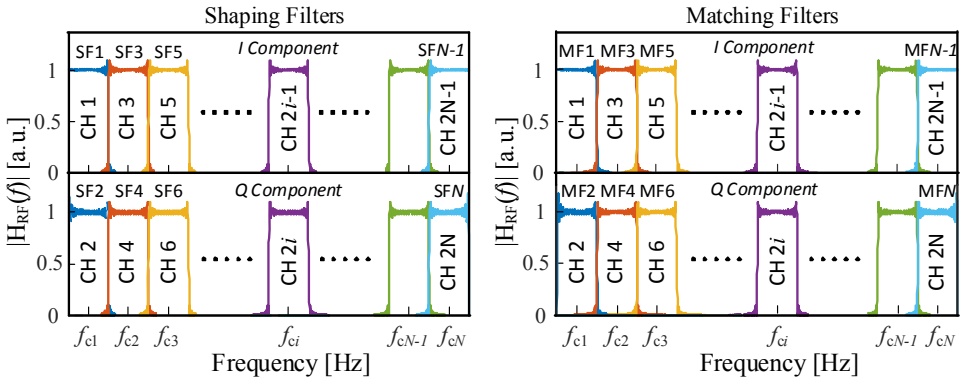

Fig. 2. Frequency responses of Hilbert-pair-based digital orthogonal shaping/matching filters and the gapless multiplexing/demultiplexing of N independent signal channels. The total number of channels is N, which is equal to the oversampling factor of M. SF: shaping filter; MF: matching filter; CH: channel.

An example of how various orthogonal shaping and matching filters are dynamically assigned to individual channels is illustrated in Fig. 2, where the frequency responses of the orthogonal filters at different central frequencies are plotted. It is also shown in Fig. 2 that the channels occupying the I and Q components of a specific filter pair share the same spectral region and there are no frequency gaps between the neighboring channels, this gives rise to an increase of spectral efficiency. From the practical network operation viewpoint, according to the end-user's demand and network traffic status which can be obtained through periodic communications between the transceiver DSP controllers and the centralized SDN network controller [13], the digital filter characteristics in each transceiver can be varied by selecting the appropriate digital filter parameters stored in the transceiver DSP controllers, this allows the dynamic allocation of optimum available filters to individual channels to be achieved online in the digital orthogonal filter space.

Optics EXPRESS

2.2 Experimental system setup

The experimental setup of the considered IMDD PON transmission systems incorporating DOF-enabled channel multiplexing/demultiplexing is illustrated in Fig. 3, where 10G class optical devices are adopted. As already stated above, digital orthogonal filtering is inherently transparent to signal modulation format. Here OFDM is utilized to encode the user information due to its high spectral efficiency and DSP richness. Meanwhile, for simplicity but without losing any generality, six independent channels are considered in the experimental demonstrations.

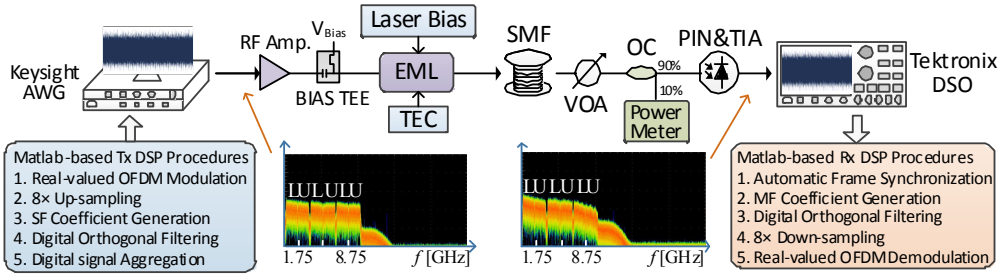

Fig. 3. Experimental system setup of digital orthogonal filtering-enabled 6-channel IMDD PON transmission system. AWG: arbitrary waveform generator; Amp: amplifier; EML: electro-absorption modulated laser; TEC: thermo-electric cooler; VOA: variable optical attenuator; OC: optical coupler; SMF: single-mode fiber; PIN&TIA: photodetector with integrated transimpedance amplifier; DSO: digital sampling oscilloscope. The insets are measured electrical signal spectra output from the AWG and PIN. L: lower sideband; U: upper sideband.

As seen in Fig. 3, at the transmitter a Matlab program is employed to perform the transmitter DSP procedures off-line, which consist of the following core processes: generation of six independent real-valued OFDM channels, 8 × up-sampling process, shaping filter coefficient calculation, digital orthogonal filtering of each individual channel, and direct digital sample summation of the six digitally filtered channels. After carrying out the transmitter DSP procedures in Matlab, the summed samples are first uploaded onto an arbitrary waveform generator (AWG) operating at 28GS/s and then converted into an analog waveform with a 10.5GHz bandwidth. A RF amplifier sets the voltage of the generated analog signal at $1.6V_{pp}$ for combination, via a bias-T, with an optimum DC bias of –0.7V. Afterwards, the resulting RF signal is used to drive a 10GHz electro-absorption modulator (EAM) within an electro-absorption modulated laser (EML), in which a 1550nm distributed feedback (DFB) laser is biased at a DC current of 125mA. Finally, the modulated optical signal from the EML is directly launched into a MetroCor SMF transmission link with an input optical power of ~2.7dBm. At the receiver, the received optical signal first passes through a variable optical attenuator (VOA) to control its optical power level. Following a 90/10 optical coupler (OC), the received optical signal is converted to the electrical domain by a 10GHz P type-intrinsic-N type (PIN) with integrated transimpedance amplifier (TIA) via direct detection. Finally, the received analog electrical signal is captured and digitized by a real-time digital sampling oscilloscope (DSO), and then processed offline using a receiver Matlab program. The major receiver DSP functions include signal synchronization, matching filter coefficient generation, DOF-based channel demultiplexing, 8 × down-sampling of each individual channel, and real-valued OFDM signal recovery by employing the DSP procedures identical to those reported in [20].

In the transceiver DSP programs, all the digital orthogonal filters are constructed according to the approach outlined in subsection 2.1 and the frequency responses of the shaping and matching filters assigned to six OFDM channels are similar to those presented in Fig. 2. The digital filter tap length, defined as the total number of original data samples

Optics EXPRESS

contributing simultaneously to the filtering process, is set to 32, whilst the excess of bandwidth factor, α, is kept at 0. Moreover, in generating/recovering an OFDM signal for each individual channel, adaptively bit-loaded 31 subcarriers, with signal modulation formats selected from quadrature phase shift keying (QPSK), 16-quaternatry amplitude modulation (QAM) and 32-QAM, are employed to carry a binary pseudo-random bit sequence (PRBS) with a length of 2^{15}-1. This results in a total number of 64 IFFT/FFT points for obtaining real-valued OFDM symbols via the Hermitian conjugation. A cyclic prefix ratio of 1/8 is employed and the signal clipping ratio is fixed at 13dB. A summary of the key transceiver and optical device parameters are listed in Table 1.

Table 1. Transceiver and Optical Device Parameters

Parameter	Value	Units
Channel number	6	/
Up-sampling factor	8	/
Digital filter tap length	32	/
Excess of the bandwidth (α factor)	0	/
Signal bandwidth per channel	3.5	GHz
Information-bearing subcarriers per channel	31	/
IFFT/FFT points per channel	64	/
Adaptive modulation format	QPSK, 16-QAM, 32QAM	
Cyclic prefix	1/8	/
Clipping ratio	13	dB
EML laser operation wavelength	~1550	nm
3dB EML modulation bandwidth	10	GHz
EML bias current	125	mA
EAM bias voltage	–0.7	V
EML laser output power	~2.7	dBm
SMF fiber type	MetroCor	
PIN detector bandwidth	10	GHz
PIN detector sensitivity[1]	–19	dBm

[1] Corresponding to 10 Gb/s non-return-to-zero data (PRBS 2^{31}-1) at a BER of 1.0×10^{-9}.

3. Experimental Results

To experimentally demonstrate the achievable transmission performance of the DOF-multiplexed multi-channel IMDD PON systems, in Subsection 3.1 the adaptively optimized signal characteristics of each individual channel are first presented in terms of their adaptive bit loading profiles and their relative electrical channel power levels. The optimizations of these parameters pave a solid path to the successful experimental demonstrations of aggregated 30.078Gb/s multi-channel IMDD PON transmissions over 10G-class optical device-based 25km SMF links described in Subsection 3.2. In addition, the transmission performances of the considered systems are also experimentally explored in Subsection 3.3 for various transmission distances up to 45km.

3.1 Optimized signal characteristics of each individual channel

To effectively reduce the impacts of the overall system frequency response roll-off effect on signal transmission performances, parameter optimizations of each individual channel are first conducted via adaptive bit loading for all information-bearing subcarriers. Moreover, adaptive channel power loading is also applied by redistributing the available electrical signal power among all of the channels.

Optics EXPRESS

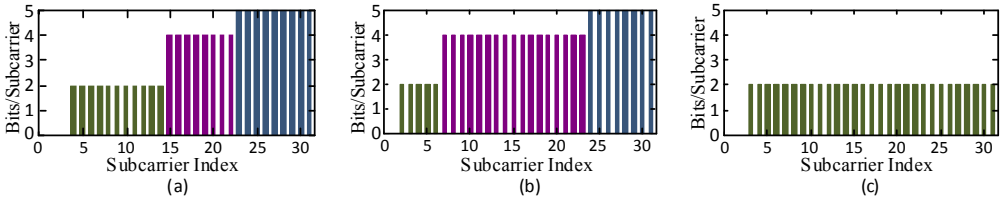

Fig. 4. Optimized adaptive subcarrier bit loading profiles for various channels. (a) CH1 and CH2; (b) CH3 and CH4; (c) CH5 and CH6.

For a considered 25km SMF IMDD PON link incorporating the 10G-class optical devices subject to the operating conditions listed in Table 1, the resulting optimum subcarrier bit allocation profiles measured for each individual channel are presented in Fig. 4. It can be seen in Fig. 4 that for two spectrally-overlapped channels occupying the same spectral region, identical bit allocation profiles are obtained. This is because these two channels experience a similar system frequency response roll-off, which is mainly determined by the chromatic dispersion-induced power fading effect associated with the IMDD system [21]. The channels located in the high-frequency spectral region suffer from the relatively strong power fading effect, as depicted in the measured spectra inserted in Fig. 3, thus only the low signal modulation format (QPSK) can be assigned to the last two channels (CH5 and CH6). It can also be seen in Figs. 4(a) and 4(b) that, for a specific signal channel, higher signal modulation formats are taken on high-frequency subcarriers. This is because the DOF process produces a double sideband spectrum with the original signal spectrum mapped to both the upper and lower sidebands, as shown in the spectra inserted in Fig. 3. The channel roll-off effect introduces amplitude variations between the corresponding frequency components in the upper and lower sidebands, this prevents full cancellation between the sidebands of the unwanted signal when these sidebands are mapped back in the receiver. As such, the cross-channel interference (CCI) effect occurs [14,15]. In particular, a larger system frequency response roll-off causes a greater amplitude variation between the two sidebands, thus lower frequency subcarriers suffer more CCI, leading to the utilization of low signal modulation formats on these subcarriers to obtain the acceptable bit error rate (BER) performances, as observed in Figs. 4(a) and 4(b). Furthermore, because the finite tap length-induced digital filter frequency response ripples are more pronounced at the low-frequency region and as large ripples give rise to the occurrence of excessive errors on the subcarriers, for each individual channel, the first several subcarriers must be dropped. Finally, the unwanted square-law photon detection-induced intermixing frequency products also slightly increases the number of dropped subcarriers for low-frequency channels (CH1 and CH2).

Table 2. System Parameters for Each Individual Channel

Channel index	Central Frequency [GHz]	Total data-carrying subcarriers	Relative power ratio[1] [dB]	Raw signal bit rate [Gb/s]
1	1.75	28	0	5.414
2	1.75	28	0	5.414
3	5.25	30	1.15	6.453
4	5.25	30	1.15	6.453
5	8.75	29	2.56	3.172
6	8.75	29	2.56	3.172
Total	/	/	/	30.078

[1] Normalized to the power of channel 1.

Based on Fig. 4 and the transceiver parameters listed in Table 1, it is easy to calculate the achieved signal bit rates of individual channels, which are presented in Table 2, thus an aggregated raw signal transmission capacity is 30.078Gb/s. In order to minimize receiver sensitivity differences between all the considered channels, it is also necessary to employ adaptive channel power allocations before multiplexing these signal channels in the digital domain. Such channel power allocation can be quantified by the power ratio between a

Optics EXPRESS

specific channel and CH1. As listed in Table 2, the optimum signal power ratios for CH3/CH4 and CH5/CH6 are 1.15dB and 2.56dB respectively. It is interesting to note in Table 2 that when the optimum bit loading and channel power loading are adopted, the transmission capacities of the signal channels located in the two low spectral bands are similar, suggesting that the achievable channel transmission capacity is mainly determined by the power fading effect of the transmission link rather than the digital filter frequency response characteristics.

3.2 25km SMF Transmission Performances

In this subsection, experimental measurements are undertaken of 30.078Gb/s DOF-multiplexed 6-channel transmission performances over the IMDD 25km MetroCor SMF PON link. Here the optimum bit loading profiles presented in Fig. 4 are employed, and the optimum device operating conditions specified in Table 1 are also adopted together with the optimized channel power levels listed in Table 2.

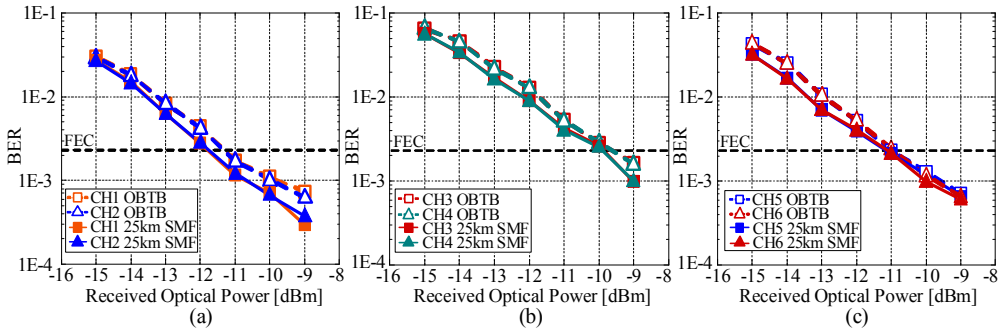

Fig. 5. Measured BER versus received optical power performances of each individual channel in a 25km SMF IMDD transmission system. (a) CH1 and CH2; (b) CH3 and CH4; (c) CH5 and CH6.

For both the optical back-to-back (OBTB) and entire IMDD 25km SMF link, Fig. 5 presents the measured BER performances of each individual channel as a function of received optical power (ROP). As expected from the theoretical predictions [13], it is shown in Fig. 5 that across the entire ROP dynamic range, the BER developing trends are very similar for all the signal channels considered. This indicates that the operation performances of DOF-based channel multiplexing/demultiplexing are independent of not only the digital filter type but also the channel spectral location. As also seen in Fig. 5, in comparison with the other channels located in different spectral regions, for CH3 and CH4, receiver sensitivity decreases of about 1.8dB are observed at a forward error correction (FEC) limit of 2.3×10^{-3} for the OBTB case. Such receiver sensitivity differences are mainly contributed by the co-existence of the limited dynamic range of the channel power ratio and the high signal bit rate conveyed by CH3 and CH4. More importantly, it should also be noted in Fig. 5 that compared to the OBTB case, a negative power penalty of >0.2dB at the adopted FEC limit occurs for each individual channel after a 25km MetroCor SMF transmission. The observed performance improvements after 25km fiber transmissions imply that the MetroCor SMF-introduced negative dispersion can compensate for the positive transient frequency chirp associated with the adopted EAM [22].

Optics EXPRESS

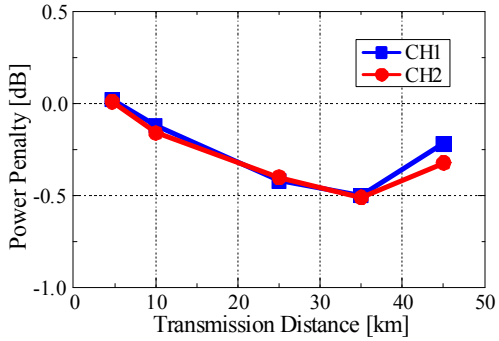

Fig. 6. Power penalty versus transmission distance for CH1 and CH2.

To further confirm the observed negative power penalty behaviors, the measured channel power penalty against MetroCor SMF transmission distance is illustrated in Fig. 6, where only CH1 and CH2 are considered to minimize the impacts of the transmission distance-dependent power fading effect and the limited optical device bandwidths on the system performance. In measuring Fig. 6, the adopted experimental conditions are identical to those used in Fig. 5, except that the transmission distance varies from 5km to 45km. It is shown in Fig. 6 that when the transmission distance increases from 5km to 35km, the negative power penalty rises due to the improved compensation of the EAM-associated frequency chirp effect [22]. On the other hand, for a transmission distance larger than 35km, the relatively sharp decrease of the negative power penalty occurs because the EAM-associated frequency chirp is over-compensated by the accumulated large chromatic dispersion effect. As a direct result of an optimum compensation between the EML frequency chirp and the accumulated chromatic dispersion, a maximum negative power penalty can be obtained at a transmission distance of 35km.

After having performed channel equalization in the receiver, the subcarrier constellations corresponding to the highest signal modulation formats taken on each individual channel are exemplified in Fig. 7, where the constellations are recorded at a ROP of −9dBm after 25km MetroCor SMF transmissions.

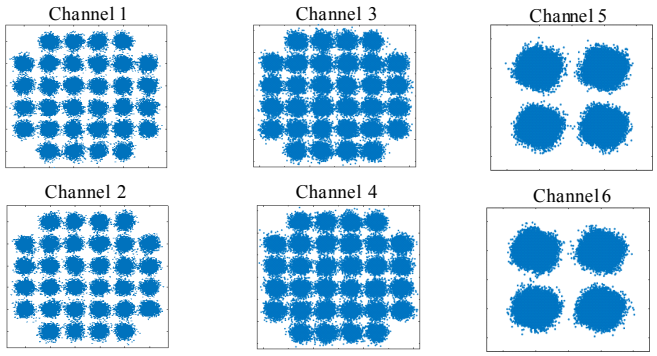

Fig. 7. Equalized subcarrier constellations for various channels at a ROP of −9dBm.

3.3 45km SMF Transmission Performances

As a direct result of the transmission distance-dependent negative power penalty shown in Fig. 6, it is straightforward to expect that the transmission performance of the considered system is also robust to variations in transmission distance. Such performance robustness can be greatly beneficial to the seamless convergence of various access networks with largely diversified design characteristics. To verify such an expectation, for an IMDD 45km

Optics EXPRESS

MetroCor SMF transmission system, the measured BER versus ROP performances of each individual channel are plotted in Fig. 8, in obtaining this figure, in comparison with Fig. 5, only the channel power level of each individual channel is optimized and no other alterations are made to device/transceiver/system parameters.

As seen in Fig. 8, compared to Fig. 5, just simple channel power allocation can enable similar BER developing trends for the involved channels, regardless the long transmission distance-enhanced power fading effect. This indicates that adaptive channel power loading can provide the DOF-multiplexed multiple channel PON systems with excellent performance robustness to transmission distance. In comparison with Fig. 5, it is also found in Fig. 8 that for CH1, the negative power penalty decreases by 0.3dB. Whilst the negative power penalties of CH6 remain almost the same for both the 25km and 45km cases. The physical mechanisms underpinning the observed channel spectral location-dependent variations in power penalty is that, compared to the low-frequency channels, the high-frequency channels experience much stronger EAM-associated frequency chirp, which inevitably requires a larger accumulated chromatic dispersion for an optimum compensation. Finally, after 45km fiber transmissions, a receiver sensitivity variation of <0.5dB is obtained at the adopted FEC limit for all the six channels, this results from the co-existence of the power fading effect and the interplay between chromatic dispersion and EAM-associated frequency chirp.

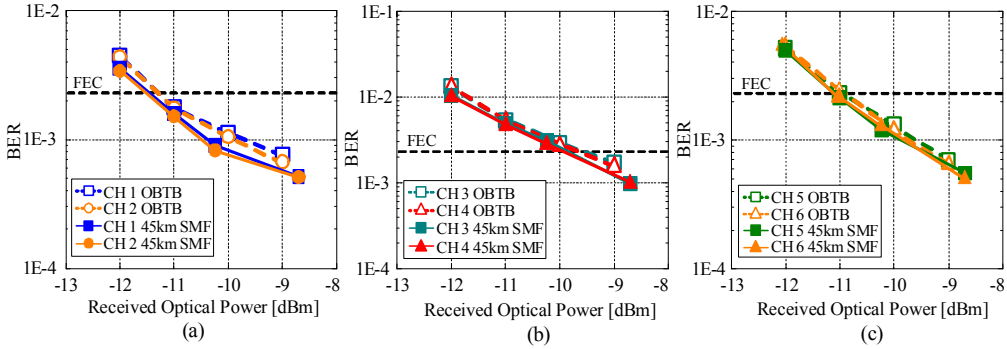

Fig. 8. BER versus received optical power performances after 45 km SMF transmissions. (a) CH1 and CH2; (b) CH3 and CH4; (c) CH5 and CH6.

4. Conclusions

By making use of off-the-shelf and low-cost 10G-class optical devices, aggregated 30.078Gb/s/λ over 25km SMF multi-channel transmissions have been experimentally demonstrated, for the first time, in IMDD PON systems incorporating DOF-multiplexed six independent channels. The experimental results have shown that by employing adaptive channel power allocation, the channel spectral location-independent transmission performance with a negative power penalty of >0.2dB is obtainable for all the involved channels. Furthermore, excellent performance robustness of the demonstrated system has also been observed for various transmission distances up to 45km. This work demonstrates the great potential of the DOF-multiplexing technique for enabling integrated cloud access networks for the seamless convergence of traditional optical access networks, metropolitan area networks and mobile fronthaul/backhaul networks.

Funding

This work was supported in part by The Ser Cymru National Research Network in Advanced Engineering and Materials (NRN024 and NRN147), and in part by Commonwealth Scholarship Commission.